Contribution from the Departments of Chemistry, The Florida State University, Tallahassee, Florida 32306, and The University of Chicago, Chicago, Illinois 60637

Oxidation of Octaaza Macrocyclic Complexes of Nickel(II): Structures Containing the New β-Diazonato Chelate Ring

GUY C. GORDON, SHIE-MING PENG, and VIRGIL L. GOEDKEN*[1]

Received July 26, 1978

The octaaza bis-α-diimine macrocyclic complex $[Ni(C_{10}H_{20}N_8)]^{2+}$, I, readily undergoes a variety of reactions involving the macrocyclic ligand. Complex I reacts with hydrazine and dioxygen via nucleophilic attack of hydrazine on an imine carbon of each five-membered ring and oxidative dehydrogenation of the six-membered rings to yield the dodecaaza complex $[Ni(C_{10}H_{20}N_{12})]$, III. The reaction of I with borohydride, followed by aerial oxidation, yields an isomer of $[Ni(C_{10}H_{18}N_8)]$, II, in which the α-diimine functions have been reduced and double bonds introduced into the six-membered rings. Initial attempts to oxidize this species to the dihydrooctaaza[14]annulene complex using the trityl cation led instead to electrophilic substitution on the six-membered rings to yield $[Ni(C_{10}H_{16}N_8(CPh_3)_2)]$, V. Complex V can be oxidized to the ditrityldihydrooctaaza[14]annulene VII, which is monomeric unlike the unsubstituted Ni–Ni bonded dimer IV. Methyl groups on the methine carbons of the six-membered rings, as in IX, block electrophilic attack by the trityl cation allowing oxidation to the dimethyldihydrooctaaza[14]annulene XI. Spectroscopic and electrochemical evidence show that the Ni^{II} ion and the trityl substituents in VII stabilize a different resonance isomer of the macrocycle than does the cobalt(III) alkyl in XIV. X-ray crystal structures of II and III have been determined to fully elucidate the delocalization patterns in the altered macrocyclic ligands. Crystal data for III, $[Ni(C_{10}H_{20}N_{12})]$: space group $P2_1/c$, $a = 9.287$ (2) Å, $b = 13.608$ (4) Å, $c = 12.565$ (4) Å, $\beta = 106.09$ (2)°, $\rho_{exptl} = 1.59$ g/cm^3, $\rho_{calcd} = 1.55$ g/cm^3, $Z = 4$. Crystal data for II, $[Ni(C_{10}H_{18}N_8)]$: space group $P2_1/c$, $a = 6.954$ (2) Å, $b = 12.594$ (3) Å, $c = 8.516$ (2) Å, $\beta = 108.43$ (2)°, $\rho_{exptl} = 1.46$ g/cm^3, $\rho_{calcd} = 1.46$ g/cm^3, $Z = 2$. The structure of II contains two saturated five-membered chelate rings and two fully delocalized, anionic six-membered chelate rings of the previously unknown β-diazonato type. The average Ni–N distance is 1.790 (3) Å and the nickel atom is crystallographically required to be in the N_4 plane. Structure III has a hydrazine adduct attached to a carbon atom of each five-membered chelate ring. Both hydrazines are located on the same side of the macrocyclic ligand plane. Two patterns of delocalization are observed in the complex. One is a fully delocalized six-membered ring of the β-diazonato type observed in structure II. The other consists of a seven-atom system extending through a delocalized allylic-like anion in the six-membered ring and an imine function in each five-membered ring. By the chemical transformations presented, three oxidation states of the octaaza macrocycle show eight patterns of unsaturation.

Introduction

One of the more intriguing aspects of macrocyclic ligand complexes of transition metals is the extent to which the ligand can be modified. In principle the ligands may be subjected to any modification within the limits of the functional groups from which they are constituted. However, the coordinated metal ions significantly alter both the course and the ease of these reactions. The most common type of reaction studied has been oxidative dehydrogenation of saturated C–N linkages.[2-10] Other reaction types that have been reported include (1) oxidative dehydrogenation of C–C bonds,[2] (2) simple deprotonation of the ligand,[11] (3) reduction of imine bonds,[12] (4) attack of nucleophiles on coordinated imine bonds,[13,14] and (5) electrophilic substitutions on unsaturated six-membered rings.[15] Most of these reactions have counterparts with metal complexes of simpler nonmacrocyclic chelate ligands.[16-22] However, the robust constitution of most synthetic macrocyclic ligands permits the above reactions to occur with greater facility than with noncyclic counterparts because these complexes may be subjected to much harsher reaction conditions.

The octaaza macrocyclic complex I is remarkable with respect to the variety of reactions which it undergoes. The nature of some of these reactions is illustrated in Scheme I. Some of these and other reactions have been described in previous publications.[23-26] This paper presents an account of the synthesis and structural characterization of the nickel(II) complexes shown in the scheme.

Experimental Section

All solvents and chemicals were obtained commercially and were reagent grade. Solvents were used without further purification other than drying over 3A molecular sieves. Infrared spectra were recorded on a Beckman IR-10 or a Perkin-Elmer 521 spectrophotometer in the range 4000–500 cm^{-1}. Samples were prepared as Nujol mulls and were calibrated with the 2851.5- and 1601.3-cm^{-1} absorptions of polystyrene film. Ultraviolet and visible spectra were obtained using a Cary Model 14 recording spectrophotometer within the range 1000–270 nm. Proton magnetic resonance spectra were recorded on either Varian A-60 or Bruker 270-MHz instruments. Elemental analyses were determined commercially by Galbraith Laboratories, Inc., Knoxville, Tenn. Electron paramagnetic resonance was performed on a Varian E12 spectrometer.

Electrochemical measurements were performed using a Princeton Applied Research Model 175 universal programmer and Model 173 potentiostat. The experiments were performed in a three-compartment glass cell with fritted-glass dividers. The central compartment was kept under a nitrogen or argon atmosphere and contained a platinum electrode. The reference electrode was a silver foil in 0.100 M $AgClO_4$ in acetonitrile connected to the reference compartment by an asbestos wick. All measurements were made in reagent grade acetonitrile dried over 3A molecular sieves, made 0.1 M in tetraethylammonium perchlorate, and deaerated with nitrogen.

Syntheses. $[Ni(C_{10}H_{20}N_{12})]$, III. A solution of 2 g of $[Ni(C_{10}H_{20}N_8)](ClO_4)_2$,[24] I, was kept under 2 atm of O_2. Hydrazine, 0.3 mL, was injected and the color of the solution became orange-red. The cherry red product started precipitating in 30 min. The product was filtered after standing overnight, washed with methanol, and dried in air. The yield was 40%. Anal. Calcd: C, 32.72; H, 5.45; N, 45.81. Found: C, 33.59; H, 5.41; N, 43.06.

$[Ni(C_{10}H_{18}N_8)]$, II. To a deaerated suspension of 510 mg (1 mmol) of I in 25 mL of methanol was added 155 mg (4 mmol) of $NaBH_4$. Within 2 min everything dissolved and gas evolution ceased. Oxygen was bubbled through the solution for about 1 min until no more heat was evolved and the color turned deep blue. Water was added dropwise until the product precipitated. The yield was 70%. The product was recrystallized from diethyl ether by the addition of methanol and water. Anal. Calcd: C, 38.87; H, 5.83; N, 36.28. Found: C, 38.99; H, 5.94; N, 36.21.

$[Ni(C_{10}H_{16}N_8(CPh_3)_2)]$, V. To a solution of 1.2 g (4 mmol) of II in 15 mL of CH_3CN was added 2.6 g (8 mmol) of Ph_3CBF_4. The solution became blue-green and the product started crystallizing within a few minutes. After 0.5 h, the product was filtered, washed with methanol, and air-dried. The yield was 70%. Anal. Calcd: C, 72.63; H, 5.80; N, 14.12. Found: C, 73.49; H, 5.85; N, 14.37.

$[Ni(C_{10}H_{12}N_8(CPh_3)_2)]$, VII. Oxygen was bubbled slowly through a boiling solution of 200 mg of V in 15 mL of toluene. After 12 h, the solution had changed color from blue-green to deep emerald green. Methanol (5 mL) was added, and, on cooling, the product crystallized as large dark green needles. The yield was 85%.

Reduction of VII to V. A deaerated solution of VII in tetrahydrofuran was treated with a large excess of $NaBH_4$ and refluxed under nitrogen until the green solution turned violet (5 min). At this

0020-1669/78/1317-3578$01.00/0

Scheme I

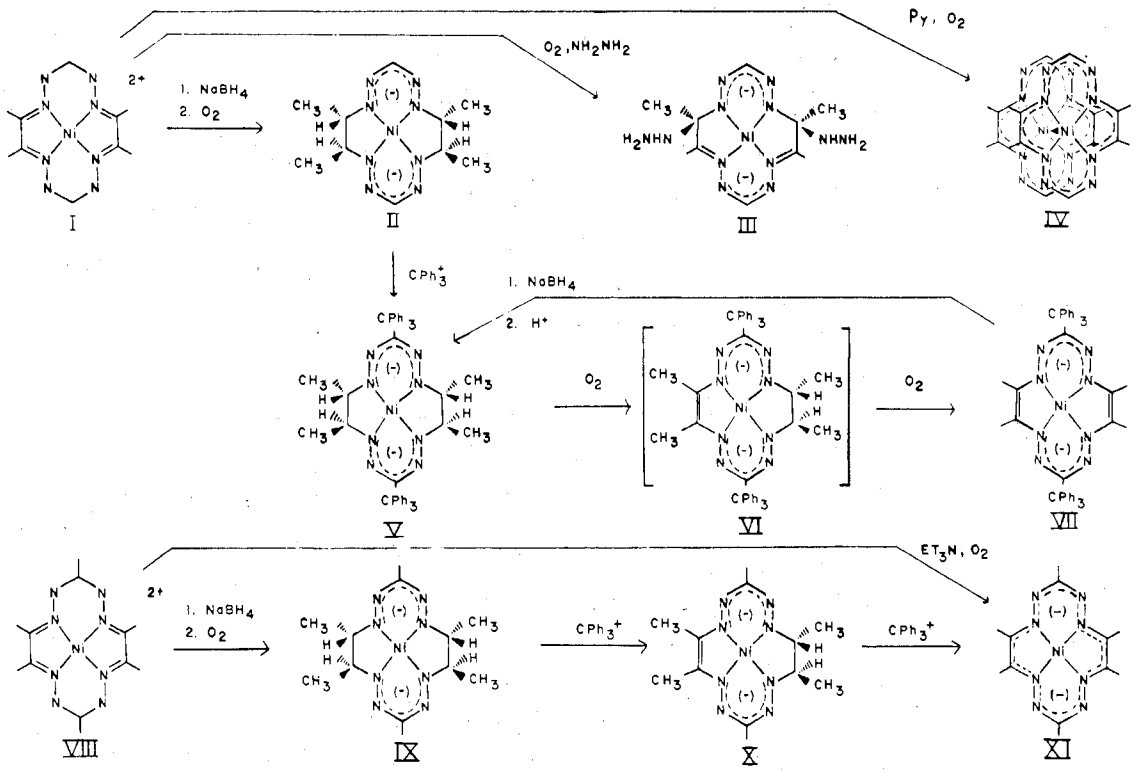

point oxygen will regenerate the green VII. Deaerated 60% $HClO_4$ was cautiously added dropwise until the color changed to blue-green. Water was added dropwise until the product, V, crystallized as blue-green needles. The yield was quantitative.

$[Ni(C_{10}H_{16}N_8(Me)_2)]$, IX. To a deaerated solution of 538 mg (1 mmol) of $[Ni(C_{10}H_{18}N_8(Me)_2)](ClO_4)_2$,[24] VIII, in 100 mL of methanol was added 155 mg (4 mmol) of $NaBH_4$. The solution was warmed slightly to ensure complete reaction as indicated by the change in color from dark brown to light brown. Oxygen was bubbled through the warm solution until no more heat was generated. The color of the solution turned burgundy red. Water (50 mL) was added and the solution was warmed again, turning green in color. The product precipitated as blue-green flakes. The crude product was extracted into diethyl ether. The ether layer was washed twice with water and once with brine and then predried over $CaCl_2$. Acetonitrile (50 mL) was added to the solution and the ether was removed on a rotary evaporator. This solution was dried over 3A molecular sieves for 24 h. The volume of the solution was then reduced on a rotary evaporator until crystals formed. The yield was 40%.

$[Ni(C_{10}H_{14}N_8(Me)_2)]$, X. To a solution of 169 mg (0.5 mmol) of IX in 25 mL of CH_3CN was added 180 mg (0.5 mmol) of Ph_3CBF_4 giving a brown solution. After 5 min, 5 mL of methanol was added to remove any unreacted Ph_3CBF_4. The solution was heated allowing 10 mL of the solvent to boil off. Diethyl ether (150 mL) was added, and the ether solution was washed with water until the water layer was no longer brown leaving a bright green solution. This solution was worked up in the same manner as X above. The yield was 30%.

$[Ni(C_{10}H_{12}N_8(Me)_2)]_2$, XI. Air was allowed to slowly diffuse into a solution of 200 mg of VIII in deaerated CH_3CN and 0.5 mL of NEt_3. The product precipitated as black microcrystals. The yield was 50%. Alternately, IX or X may be oxidized by excess Ph_3CBF_4 or air.

Growth of Single Crystals for Structural Investigation. Ruby red crystals of $[Ni(C_{10}H_{20}N_{12})]$, pseudooctahedrally shaped and suitable for X-ray investigation, were obtained after numerous recrystallizations of the compound from trifluoroethanol. Long, thin, blue-black needle-like crystals of $[Ni(C_{10}H_{18}N_8)]$ having highly reflective faces were grown by slow diffusion of water into an acetonitrile solution of the compound.

Details of the X-ray Structure Determination

Crystal Examination and Data Collection. X-ray precession photographs of $[Ni(C_{10}H_{18}N_8)]$ and $[Ni(C_{10}H_{20}N_{12})]$ exhibited monoclinic symmetry with systematic absences consistent with the unique space group $P2_1/c$.[27] Lattice constants and their estimated standard deviations, together with other pertinent crystal data, are given in Table I. The details of the data collection for both complexes are also presented in Table I.[28] The data were reduced in the conventional manner with corrections applied for Lorentz and po-

Table I. Crystal Data and Data Collection Details

compd	$[Ni(C_{10}H_{20}N_{12})]^0$	$[Ni(C_{10}H_{18}N_8)]^0$
mol wt	376.06	309.02
space group	$P2_1/c$	$P2_1/c$
a, Å	9.287 (2)	6.954 (2)
b, Å	13.608 (4)	12.594 (3)
c, Å	12.565 (4)	8.516 (2)
α, deg	90.0 (0)	90.00 (0)
β, deg	106.09 (2)	108.43 (2)
γ, deg	90.0 (0)	90.00 (0)
Z	4	2
no. of reflections used to determine cell constants	24	25
2θ limits, deg	$60 \leq 2\theta \leq 70$ (Cu Kα)	$30 \leq 2\theta \leq 40$ (Mo Kα)
d_{calcd}, g/cm^3	1.59	1.46
d_{exptl}, g/cm^3	1.55	1.46
absorption coeff, cm^{-1}	19.61	13.75
crystal dimension, mm	0.25 × 0.25 × 0.25	0.09 × 0.09 × 0.5
absorption cor	NO	NO
diffractometer	Picker-FACS-1	Picker-FACS-1
monochromater (Bragg angle)	NO	graphite (6.093)
λ (Kα), Å	1.5418 (Cu)	0.710 69 (Mo)
Takeoff angle, deg	0	3.0
method	θ–2θ	θ–2θ
scan speed, deg/min	1.0	2.0
scan width, deg	2.0	1.8
bkgd time	20 × 2	20 × 2
standards	3	3
av med dev of standards, %	1	2 (random)
2θ limits of data, deg	$0 \leq 2\theta \leq 130$	$0 \leq 2\theta \leq 55$
no. of data collected	2868 (non-std) 2570 (unique)	1856 (non-std)
no. of data used in final refinement	2109 ($F > 3\sigma(F)$)	1394 ($F > 3\sigma(F)$)

Table II. Summary of the Details of the Solution and Refinement of the Structures

compd	$[Ni(C_{10}H_{20}N_{12})]^0$	$[Ni(C_{10}H_{18}N_8)]^0$
method	heavy-atom techniques	heavy-atom techniques
heavy atom position from Patterson synthesis	general position: $x = 0.195$, $y = 0.114$, $z = 0.103$	special position: $x = 0.0$, $y = 0.0$, $z = 0.0$
problem in refinements	yes[a]	no
no. of cycles used in refinements	8	5
model for final cycle of refinement	all nonhydrogen atoms positional and anisotropic thermal parameters varied; hydrogen atoms included as fixed contributions	all nonhydrogen atoms positional and anisotropic thermal parameters varied; hydrogen atoms included as fixed contributions
final R_1[b]	5.9	3.5
final R_2[b]	4.7	3.8
highest peak (e/Å^3) in final difference Fourier map	0.7 around disordered portion	0.4 around Ni
noise level of final Fourier map, e/Å^3	<0.25	<0.20
ratio of observations to variables	9.4:1	15.8:1

[a] Problem discussed in text. [b] $R_1 = \Sigma[||F_o| - |F_c||]/\Sigma|F_o|$; $R_2 = \{\Sigma w[|F_o| - |F_c|]^2/\Sigma w|F_o|^2\}^{1/2}$.

larization effects. Estimated standard deviations of the reflection intensities and derived F's based primarily on counting statistics were calculated using the equation

$$\sigma(I) = \left[S + \frac{T_s^2(B_1B_2)}{T_B^2(B_1 + B_2)} + (pS)^2 \right]^{1/2}$$

S, B_1, and B_2 are the accumulated counts for the scan and two backgrounds, T_s and T_B are the scan and individual background counting times, and p is a factor,[29] here taken to be 0.02, to account for machine fluctuations and other factors which would be expected to cause variations proportional to the reflected intensity. The F^2's and F's were calculated in the usual way from the intensities, and the $\sigma(F)$'s were calculated using the approximation

$$\sigma(F) = \sigma(I)/2F(Lp)^{1/2}$$

A total of 2129 independent reflections with $F \geq 2\sigma(F)$ was used in the refinement of $[Ni(C_{10}H_{20}N_{12})]$ and 1394 data with $|F| > 3\sigma(F)$ were used for $[Ni(C_{10}H_{18}N_8)]$. The effects of absorption (μ = 19.61 and 13.75 cm^{-1} for $[Ni(C_{10}H_{20}N_{12})]$ and $[Ni(C_{10}H_{18}N_8)]$, respectively) were judged to be minimal for the particular crystals used and were not compensated for.

Structural Solution and Refinement of the Structures. Both structures were solved by standard heavy-atom methods and refined by full-matrix least-squares techniques.[30] Scattering factors of neutral atoms were taken from standard sources.[31] Corrections for anomalous dispersion were applied to the nickel atom of each structure from the values of $\Delta f'$ and $\Delta f''$ tabulated by Cromer. The details of the solution and refinement of the structures are summarized in Table II. The solution and refinement of $[Ni(C_{10}H_{18}N_8)]$ were straightforward.

The initial solution for the structure of $[Ni(C_{10}H_{20}N_{12})]$ appeared straightforward with all of the atoms being located on the first Fourier map. Two cycles of refinement employing anisotropic temperature factors for the nickel atom and isotropic temperature factors for the nonhydrogen atoms yielded R_1 = 6.8% and R_2 = 8.1% for the 1033 most intense data. Although the bond distances and angles involving the nickel atom and the 14 atoms of the macrocyclic ring were consistent with those expected at this degree of refinement, those of the substituents (methyl groups and hydrazine moieties) of C3 and C5 were chemically unreasonable. Careful examination of a difference Fourier map obtained at this point revealed disorder between the meso and *d,l* configurations of atoms C3 and C5 as determined by the orientation of the methyl and hydrazine substituents. One cycle of full-matrix refinement in which the minor fragments of the disordered hydrazines (DN9, DN10, DN11, and DN12) were included, varying the multiplicities in addition to the isotropic temperature factors and the positional parameters, yielded residuals of R_1 = 4.8% and R_2 = 5.1% using the most intense 1033 data. Eight hydrogen atoms attached to C1, C4, C7, and C10 were located from a difference Fourier map; their positions were optimized to normal geometry for these systems and were then included as fixed contributions in the remaining cycles of refinement. Hydrogen atoms in the disordered portions of the structure could not be located.

Continued refinement with 2109 data having $|F| \geq 3\sigma(F)$ and using anisotropic thermal parameters for all atoms was unsuccessful because some temperature factor terms of the disordered hydrazine atoms DN9 and DN11 became negative. However, a difference Fourier map indicated that the electron density of these atoms was well accounted for by the anisotropic thermal motions of C8, C9, N9, and N11. The final model included only atoms DN10 and DN12 from the disordered portion. The positional parameters and anisotropic thermal parameters of all nonhydrogen atoms were varied, in addition to the multiplicities of all atoms involved in the regions of disorder. At convergence, R_1 = 5.9% and R_2 = 4.7%. The highest peak on the final difference Fourier map corresponded to 0.7 e/Å^3 and was located in the vicinity of the disordered atoms. The multiplicities of the disordered fragments were not equal for the two halves of the molecule; the multiplicity of DN10 was 0.36 and that of DN12 was 0.13. Since the major interests in this structure pertain to the patterns of delocalization in the macrocyclic ligand, the disorder of the hydrazine and methyl substituents, though unfortunate, does not seriously affect the sought after structural results.

The final positional and thermal parameters of the nonhydrogen atoms for $[Ni(C_{10}H_{18}N_8)]$ are listed in Table III and those for $[Ni(C_{10}H_{20}N_{12})]$ are listed in Table IV. Hydrogen atom positions for the two structures are listed in Tables V and VI.

Results and Discussion

The octaaza macrocyclic complex I is particularly susceptible to oxidation reactions involving the N–N and C–N linkages, to nucleophilic attack on the α-diimine functions, and to hydrogenation of the imine linkages. Under certain conditions, a number of transformations occur sequentially. For example, a complicated series of reactions occur when excess

Table III. Final Positional and Thermal Parameters[a] and Their Estimated Standard Deviations in Parentheses

atom	x	y	z	β_{11}	β_{22}	β_{33}	β_{12}	β_{13}	β_{23}
Ni	0.0000 (0)	0.0000 (0)	0.0000 (0)	134.3 (10)	43.9 (3)	97.5 (6)	−1.4 (4)	14.5 (6)	5.7 (4)
N1	0.1934 (3)	0.1015 (1)	0.0371 (3)	144 (4)	46 (1)	152 (4)	2 (2)	24 (3)	9 (2)
N2	0.3318 (3)	0.1257 (2)	0.1742 (3)	156 (5)	51 (1)	201 (5)	1 (2)	−8 (4)	−15 (2)
N3	0.2415 (3)	−0.0160 (2)	0.3323 (3)	218 (6)	75 (2)	109 (3)	34 (2)	−1 (3)	−3 (2)
N4	0.0958 (3)	−0.0522 (2)	0.2083 (2)	172 (5)	56 (1)	107 (3)	11 (2)	23 (3)	10 (2)
C1	0.3663 (5)	0.1067 (3)	−0.1718 (4)	225 (8)	109 (3)	302 (8)	46 (4)	157 (7)	78 (4)
C2	0.2075 (4)	0.1585 (2)	−0.1106 (4)	181 (6)	53 (2)	216 (6)	3 (3)	66 (5)	33 (3)
C3	0.3447 (4)	0.0695 (2)	0.3105 (3)	213 (7)	65 (2)	148 (5)	14 (3)	−36 (4)	−24 (2)
C4	0.0046 (4)	−0.1539 (2)	0.2389 (3)	211 (6)	63 (2)	148 (4)	19 (3)	60 (4)	35 (2)
C5	0.1389 (4)	−0.2464 (2)	0.2289 (4)	237 (7)	65 (2)	262 (7)	20 (3)	68 (6)	43 (3)

[a] The form of the anisotropic thermal parameters is $\exp[-(h^2\beta_{11} + k^2\beta_{22} + l^2\beta_{33} + 2hk\beta_{12} + 2hl\beta_{13} + 2kl\beta_{23})] \times 10^{-4}$.

Table IV. Final Positional and Thermal Parameters[a] and Their Estimated Standard Deviations in Parentheses for $[Ni(C_{10}H_{20}N_{12})]$

atom	x	y	z	β_{11}	β_{22}	β_{33}	β_{12}	β_{13}	β_{23}
Ni	0.19544 (7)	0.11438 (5)	0.10288 (6)	71.1 (9)	48.4 (5)	49.5 (6)	−1.2 (6)	13.7 (6)	5.2 (5)
N1	0.1324 (4)	0.0194 (3)	0.1866 (3)	83 (5)	42 (2)	53 (3)	−2 (3)	18 (3)	1 (2)
N2	−0.0133 (4)	0.0018 (3)	0.1903 (3)	73 (5)	55 (3)	80 (4)	−7 (3)	25 (3)	15 (3)
N3	−0.1286 (4)	0.1327 (3)	0.0559 (3)	67 (5)	61 (3)	76 (4)	−6 (3)	15 (3)	12 (3)
N4	0.0042 (4)	0.1655 (3)	0.0392 (3)	71 (5)	45 (2)	49 (3)	−5 (3)	10 (3)	1 (2)
N5	0.2599 (4)	0.2085 (3)	0.0282 (3)	78 (5)	53 (3)	55 (3)	−3 (3)	15 (3)	2 (2)
N6	0.3951 (4)	0.2278 (3)	0.0254 (3)	96 (6)	61 (3)	76 (4)	−10 (3)	33 (4)	11 (3)
N7	0.5067 (4)	0.0979 (3)	0.1535 (3)	73 (5)	59 (3)	75 (4)	2 (3)	29 (3)	4 (3)
N8	0.3807 (4)	0.0684 (3)	0.1657 (3)	73 (5)	49 (3)	54 (3)	0 (3)	19 (3)	4 (2)
N9	0.1169 (5)	0.3767 (4)	−0.0253 (6)	155 (9)	58 (4)	122 (8)	−10 (5)	12 (5)	17 (4)
N10	0.1787 (6)	0.4048 (5)	0.0871 (8)	253 (13)	117 (6)	203 (13)	−39 (6)	47 (8)	19 (6)
N11	0.4987 (4)	0.0016 (3)	0.3510 (3)	129 (6)	81 (4)	67 (4)	16 (4)	5 (4)	1 (3)
N12	0.4606 (5)	0.0909 (4)	0.3987 (4)	159 (8)	81 (5)	107 (5)	18 (4)	6 (5)	−27 (3)
C1	−0.1174 (5)	0.0581 (4)	0.1258 (4)	77 (7)	64 (4)	79 (5)	−11 (4)	31 (4)	4 (4)
C2	−0.0031 (5)	0.2392 (3)	−0.0264 (4)	78 (6)	49 (3)	50 (4)	−2 (4)	5 (4)	−1 (3)
C3	0.1424 (5)	0.2740 (4)	−0.0445 (4)	95 (7)	57 (4)	74 (5)	−2 (4)	15 (4)	20 (3)
C4	0.5096 (5)	0.1733 (4)	0.0860 (4)	80 (7)	67 (4)	90 (5)	−3 (4)	32 (5)	11 (4)
C5	0.3941 (5)	−0.0160 (4)	0.2438 (4)	96 (6)	50 (3)	47 (4)	7 (4)	13 (4)	4 (3)
C6	0.2373 (5)	−0.0322 (3)	0.2519 (4)	104 (7)	45 (3)	46 (4)	−3 (4)	20 (4)	2 (3)
C7	−0.1435 (5)	0.2916 (4)	−0.0856 (4)	112 (7)	64 (4)	79 (5)	9 (4)	5 (5)	13 (4)
C8	0.1402 (6)	0.2601 (13)	−0.1652 (9)	209 (10)	190 (15)	123 (8)	39 (8)	72 (7)	71 (9)
C9	0.4513 (5)	−0.1086 (4)	0.1921 (4)	280 (10)	87 (4)	158 (6)	36 (5)	72 (6)	−10 (4)
C10	0.2114 (5)	−0.1044 (4)	0.3340 (4)	131 (8)	62 (4)	77 (4)	−3 (4)	25 (5)	16 (4)

[a] The form of the anisotropic temperature factor is $\exp[-(h^2\beta_{11} + k^2\beta_{22} + l^2\beta_{33} + 2hk\beta_{11} + 2hl\beta_{13} + 2kl\beta_{23})] \times 10^4$.

Table V. Calculated Positions of Hydrogen Atoms[a] for $[Ni(C_{10}H_{18}N_8)]$

H	attached to C	x	y	z
H1	C2	0.2422	0.2311	−0.0830
H2	C3	0.4430	0.0940	0.4086
H3	C4	−0.0088	−0.1520	0.3474
H4	C1	0.3175	0.0394	−0.2187
H5	C1	0.4867	0.0973	−0.0813
H6	C1	0.3924	0.1510	−0.2528
H7	C5	0.0767	−0.3115	0.2419
H8	C5	0.2671	−0.2398	0.3094
H9	C5	0.1560	−0.2461	0.1202

[a] All temperature factors were set at $B = 5.0$ Å^2.

Table VI. Calculated Positions of Hydrogen Atoms for $[Ni(C_{10}H_{20}N_{12})]$

H	attached to C	x	y	z
H1	C1	−0.211 78	0.039 97	0.130 36
H2	C4	0.602 99	0.189 43	0.080 04
H3	C7	−0.185 04	0.322 44	−0.032 11
H4	C7	−0.121 32	0.341 29	−0.132 27
H5	C7	−0.213 64	0.246 85	−0.128 33
H6	C10	0.110 50	−0.127 13	0.311 17
H7	C10	0.277 02	−0.159 64	0.337 88
H8	C10	0.231 03	−0.075 51	0.405 34

hydrazine is added to acetonitrile solutions of I under oxygen. An exothermic reaction occurs with nitrogen gas evolution while the color of the solution changes from orange to cherry red. The crude product from this reaction, $[Ni(C_{10}H_{20}N_{12})]$, III, apparently consists of a mixture of isomers (vide supra), and several recrystallizations were necessary to obtain a uniform-appearing product.

The usual physical methods of characterization could not be used to distinguish III from the four structural possibilities envisaged: (a) structure III with the hydrazine adducts on the same side of the macrocyclic plane, with C_s symmetry (meso form); (b) the substituent sites the same as III but with the hydrazine adducts on opposite sides of the macrocyclic plane, C_2 symmetry (*d,l* form); (c) the hydrazine substituted at positions C3 and C6 (Figure 4) and on the same side of the macrocyclic plane, C_2 symmetry (meso form); (d) substituent sites as in (c) but with the hydrazines on the opposite side of the macrocyclic plane, C_2 symmetry (*d,l* form). The IR spectrum has characteristic NH_2 absorptions at 3305, 3195, and 1580 cm^{-1}. Strong and broad absorptions in the 1300–1500-cm^{-1} region suggested several types of delocalization patterns. The NMR spectrum (Table VII) shows resonances at 1.40 ppm (6) and 2.27 ppm (6) indicative of two types of methyl groups adjacent to the hydrazines. The peak at 2.27 ppm is attributed to the methyl on the imine function. Two broad peaks at 2.93 ppm (4) and 4.33 ppm (2) correspond to the NH_2 and NH hydrogens, respectively. The C–H resonances of the six-membered rings appear at 7.39 and 8.63 ppm. The electronic spectra for all of the complexes derived from I are listed in Table VIII. The spectra for all of the complexes reported have high extinction coefficients in the visible region characteristic of charge transfer and other fully allowed transitions.

Addition of borohydride to I, followed by aerial oxidation, yields a deep blue molecular species having the composition $[Ni(C_{10}H_{18}N_8)]$, II. The proposed reduced intermediate, $[Ni(C_{10}H_{22}N_8)]^{2+}$, could not be isolated, perhaps because the large number of configurational isomers inhibit crystallization. Reoxidation of the reduced species with molecular oxygen introduces double bonds into the hydrazine linkages because N–N bonds are more easily oxidized than C–N linkages. The oxidation also eliminates some configurational isomers by eliminating the chiral nitrogen centers.

The NMR (Table VII) and IR spectra of II confirm its assigned structure. The IR spectrum is devoid of any N–H or α-diimine absorptions and a strong, intense absorption at 1280 cm^{-1} characteristic of delocalized six-membered chelate rings analogous to pentanediiminato chelate rings is present. The NMR spectrum consists of a doublet at 1.32 ppm (12) attributed to the methyl groups, a quartet at 3.47 ppm (2) assigned to the tertiary hydrogen atoms, and a singlet at 8.34 ppm (2) assigned to the methine protons of the six-membered rings. Complex II is air-stable, soluble in halocarbon solvents and acetonitrile but insoluble in water. We were unable to isolate the protonated complex as decomposition occurs in the presence of strong acids such as perchloric acid.

Attempts to extend the unsaturation of II to include the five-membered chelate rings and to produce the dimeric octaaza[14]annulene complex IV by a new route were unsuccessful. The trityl cation, which has previously been used successfully to oxidatively dehydrogenate closely related

Table VII

complex	solvent	^{1}H NMR spectrum[a]	parent peak[b] of mass spectrum	electrochemistry[c]
$[Ni(C_{10}H_{20}N_{12})]$, III	$CDCl_3$	1.40 (s, 6), 4.33 (b, 2) 2.27 (s, 6), 7.38 (s, 1) 2.93 (b, 4), 8.63 (s, 1)	not observed	
$[Ni(C_{10}H_{18}N_8)]$, II	CD_3CN	1.32 (d, 12) 7 Hz 3.47 (q, 4) 7 Hz 8.34 (s, 2)	*m/e* 308	−1.90 q 0.46
$[Ni(C_{10}H_{16}N_8(CPh_3)_2)]$, V	$CDCl_3$	1.50 (d, 12) 6 Hz 3.30 (q, 4) 6 Hz 7.24 (s, 30)	*m/e* 792	−1.92 q 0.34 1.25 i
$[Ni(C_{10}H_{12}N_8(CPh_3)_2)]$, VII	Me_2SO-d_6	2.22 (s, 12) 7.10 (s, 30)		−1.94 q 0.33 1.49 i
$[Ni(C_{10}H_{16}N_8(Me)_2)]$, IX	Me_2SO-d_6	1.23 (d, 12) 6.5 Hz 2.48 (s, 6) 3.35 (m, 4)	*m/e* 336	−1.95 q 0.25 1.24 i
$[Ni(C_{10}H_{14}N_8(Me)_2)]$, X	C_6D_6	1.35 (d, 6) 6.5 Hz 2.68 (s, 6) 3.16 (s, 6) 4.30 (m, 2)		−1.44 0.39 q 0.49 i 1.20 i 1.44 i

[a] In ppm. Numbers in parentheses refer to type of resonance (s = singlet, d = doublet, q = quartet, m = multiplet) and relative integrated intensity, respectively. [b] For ^{58}Ni. [c] q = quasi-reversible, i = irreversible.

Table VIII. Electronic Spectra for Octaaza Macrocyclic Complexes of Nickel(II)[a]

complex	absorption maxima, nm
$[Ni(C_{10}H_{20}N_{12})]$, III	552 (1.13),[b] 520 (7.98, sh[c]), 373 (13.2), 313 (9.85)
$[Ni(C_{10}H_{18}N_8)]$, II	622 (1.85), 568 (1.58, sh), 440 (1.36, sh), 300 (7.58)
$[Ni(C_{10}H_{16}N_8(CPh_3)_2)]$, V	654 (2.66), 604 (2.13, sh), 460 (0.61, sh), 310 (0.215)
$[Ni(C_{10}H_{12}N_8(CPh_3)_2)]$, VII	670 (2.8), 455 (1.4, sh), 410 (2.4), 355 (4.2, sh), 315 (9.6)
$[Ni(C_{10}H_{16}N_8(Me_2)_2)]$, IX	650 (2.00), 610 (1.72, sh), 550 (0.80, sh), 445 (0.92), 325 (5.28, sh), 295 (6.25)
$[Ni(C_{10}H_{14}N_8(Me)_2)]$, X	700 (2.87), 660 (2.52, sh), 570 (0.88, sh), 440 (4.33), 415 (4.68), 365 (6.35), 325 (5.00, sh)

[a] All solutions in acetonitrile. [b] Numbers in parentheses refer to molar extinction coefficients $\times 10^{-3}$. [c] sh = shoulder.

five-membered chelate rings,[2,9] led not to the anticipated product but rather to electrophilic substitution on the six-membered rings yielding $[Ni(C_{10}H_{16}N_8(CPh_3)_2)]$, V. The assigned structure was confirmed by the usual physical–chemical techniques. The electronic spectrum is very similar to the unsubstituted precursor II, the major difference being a red shift of all of the absorption bands. The positions of the NMR resonances of the methyl and hydrogen substituents of the five-membered rings of II and V also appear at similar frequencies indicating little difference in their electronic environments.

The differences in the reactivity between II and XII[2]

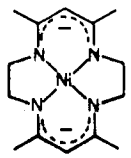

XII

toward the trityl cation may be attributed to three factors. (1) It is quite likely that the two methyl substituents of XII interfere with the addition of large bulky groups such as the trityl cation. (2) The distribution of negative charge over the two types of six-membered chelate rings undoubtedly differs, affecting their relative nucleophilicities. (3) The geometrical requirements of saturated five- or six-membered chelate rings have been shown in some instances to lead to distortions in adjacent delocalized or unsaturated chelate rings, which would otherwise be planar. The decrease in π-orbital overlap is predicted to vary as the cosine of the torsion angle.[32] Enhanced reactivity at these sites as a function of the torsion angle is expected, and unusual reactivity with deformed, delocalized six-membered chelate rings has recently been demonstrated.[33,34]

The trityl-substituted complex V is oxidized by oxygen in boiling toluene—conditions under which the unsubstituted complex II is stable for days. The intermediate oxidation product VI could not be isolated. Instead, complete oxidation gave the dirityldihydrooctaaza[14]annulene VII. Significantly, this complex is not dimeric, via a Ni–Ni bond, as is the unsubstituted complex IV. The bulky trityl groups prohibit close cofacial approach of these macrocycles. This complex is very soluble in nonpolar solvents in contrast to the near complete insolubility of IV and XI (vide infra).

An unusually facile reduction of the C=C double bonds in the five-membered rings of VII occurs in dimethyl sulfoxide, dimethylformamide, and acetonitrile solutions over a period of days, giving as sole product the precursor V. The reductant is unknown at this time but is suspected to be water. VII may be quantitatively reduced to V via borohydride. This ease of reduction is in keeping with the 16π-electron antiaromatic nature of the complex.

In order to gain understanding of the relative electronic and steric effects of the trityl substituents on the chemistry of the macrocycle, the same series of reactions was carried out on the methyl-substituted complex VIII (obtained by substituting acetaldehyde for formaldehyde in the template condensation of I). Reduction of VIII and oxidation to IX proceeds the same as for II, but in IX the methine carbons are blocked to electrophilic attack by the trityl cation. Oxidation is thus effected to X. The NMR spectrum of X clearly shows that a double bond has been introduced into one of the five-membered rings. A second equivalent of trityl cation oxidizes the remaining five-membered ring giving a black, insoluble product XI. This same product may be more easily produced in the manner of IV by oxidation of VIII in base. The mass spectrum of XI shows a parent peak at *m/e* 332 corresponding to monomeric $[Ni(C_{10}H_{12}N_8(Me)_2)]$. The insolubility of this material is consistent with extended interactions in the solid state; however, the infrared spectrum of XI is totally unlike

that of IV indicating different electronic ligand structure.

Formally, these dihydrooctaaza[14]annulene ligands are antiaromatic 16π-electron systems and localized double bonds might be predicted. However, different patterns or arrangements of delocalization are possible within the various types of chelate rings in the metal complexes. We have found that different resonance isomers of the 16π 14-membered ring may be stabilized by varying the metal ion, the coordination geometry, and the substituents of the complexes. Three X-ray structures of dihydrooctaaza[14]annulenes have been determined: IV,[41] XIII,[41] and XIV.[39] In the dimer IV, the close

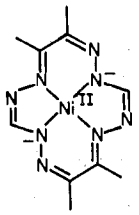

XIII

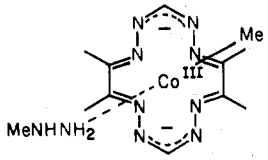

XIV

approach of the two macrocycles splits the electronic levels forming two weakly δ-bonding orbitals from the two partially filled π^* orbitals of each ligand. This removes the antiaromatic character of the ligands leaving totally delocalized π electron systems (i.e., no one resonance form predominates). In contrast, XIII, which differs from IV solely in the coordination of two different ligand nitrogens, does not dimerize and has the localized π structure shown. (Note especially that the negative charges are not delocalized over the six-membered rings.) A different resonance isomer is stabilized in the cobalt(III) alkyl complex XIV, in which conjugated α-diimines in the five-membered rings are isolated from allylic type anions in the six-membered rings. The reasons for these differences are not clear.

Complex VII is chemically identical with dimer IV except for the two trityl substituents, which prevent dimerization. The spectroscopic and electrochemical data of these complexes show VII to be a fourth resonance isomer of this ligand—isolated double bonds in the five-membered rings and delocalized 6π β-diazonato six-membered rings as in II (vide infra). Thus the four-electron oxidation of V merely incorporates C=C double bonds into the five-membered rings and involves no resonance isomerization to the alternative α-diimine form observed in XIV. The spectra and electrochemistries of II, V, VII, and IX form a smoothly varying series and are totally different from those of XIII. All four complexes show a strong IR absorption peak between 1280 and 1230 cm^{-1} attributable to the β-diazonato chelate rings. Complexes II and IX showed no α-diimine absorption around 1600 cm^{-1}; however, this absence could not be confirmed in V and VII due to trityl absorption at this energy. The intense blue and green colors of II, V, and IX arising from absorption at 622, 654, and 650 nm, respectively (Table VIII), are attributable to charge-transfer transitions involving the β-diazonato ring. This characteristic absorption is also present in VII, red shifted to 670 nm.

The electrochemistry of XIII (Figure 1) shows two reversible one-electron oxidations at 0.68 and 0.96 V and a reversible one-electron reduction at −1.42 V. This is not at all like the behavior of VII which has a single reversible one-electron oxidation at 0.33 V and a one-electron reduction at −1.94 V. Any significant resonance contribution to VII from an α-diimine structure such as in XIV is ruled out because Ni^{II} α-diimines are easily reduced to ligand radical anions.[35] Thus complexes I and VIII show pairs of one-electron reductions at −0.83, −1.24 and −0.82, −1.21 V, respectively, while VII shows no such reductions. An X-ray crystal structure is underway to verify this fourth pattern of delocalization.

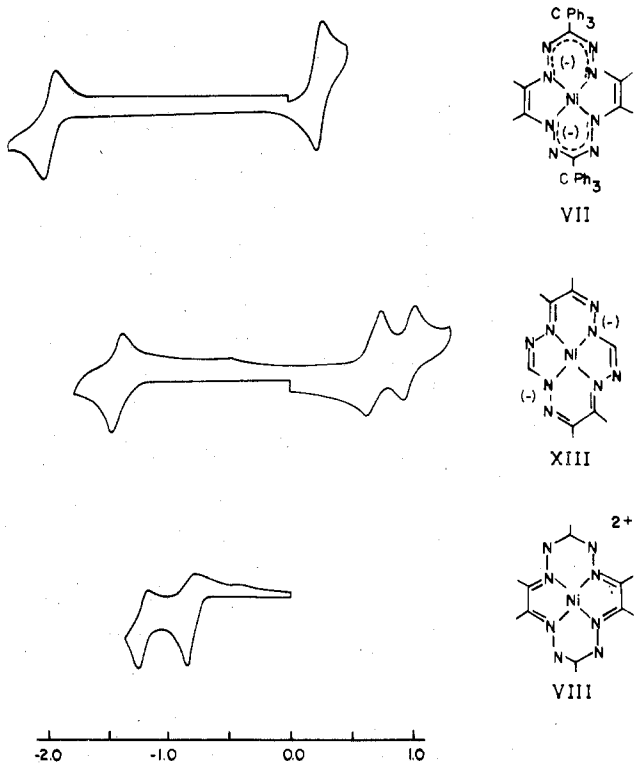

VII

XIII

VIII

Figure 1. Cyclic voltammograms for Ni^{II} complexes VII, XIII, and VIII.

The ESR spectrum of VII oxidized by $[Fe(phen)_3]^{3+}$ shows the product to be $[(Ni^{III}L)]^+$ rather than a 15π ligand-based radical cation such as that described by Holm.[2] The spectrum consists of three lines: $g_z = 2.127$, $g_x = 2.02$, $g_y = 1.990$. The ordering of $g_{x,y} < g_z$ is consistent with the unpaired electron being in the nickel d_{xy} (b_{2g}) orbital. This was shown to be the general case for Ni^{III} complexes of dianionic ligands by Busch et al.[35]

The electrochemical oxidation of the series II, V, VII, and X is easily explained in terms of oxidation to Ni^{III}. Electron-donating substituents on the methine carbons of the six-membered rings help stabilize the Ni^{III} state, making the complex easier to oxidize. Thus, replacing hydrogen with methyl (II to IX) stabilizes Ni^{III} by 0.21 V, while trityl (V) effects only a 0.12-V stabilization indicating that trityl is only 60% as electron donating as methyl relative to hydrogen. From this it may be concluded that the major effect of the trityl groups in keeping VII monomeric is steric rather than electronic. The primary effect of adding double bonds in the five-membered rings of VII is to shrink the hole size of the macrocycle, slightly stabilizing the smaller Ni^{III} ion.

Description of the Structures

The structure of $[Ni(C_{10}H_{18}N_8)]$, II, consists of an octaaza macrocyclic ligand complex of nickel(II) containing saturated five-membered chelate rings and delocalized tetraaza six-membered chelate rings. The methyl substituents of the five-membered rings are axially oriented, an arrangement which minimizes nonbonding interactions.

The molecule is illustrated by the ORTEP plot of Figure 2 which also contains the labeling scheme and selected interatomic distances and bond angles from Table IX. A stereoview of the molelcule is presented in Figure 3.

The six-membered chelate rings, although formally containing two double bonds and a negative charge, are totally delocalized, much like 2,4-pentanediiminato chelate rings. The average N–N distance, 1.293 (3) Å, is intermediate between N–N single and N=N double bonds.[36] The C–N lengths within the six-membered rings, 1.336 (4) Å, are, within ex-

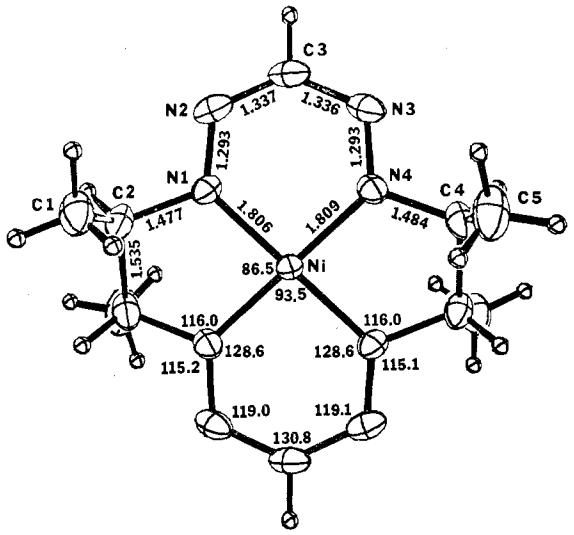

Figure 2. Molecular structure (ORTEP plot, showing 20% probability contours), labeling scheme, and selected interatomic distances and angles of the macrocyclic complex $Ni(C_{10}H_{18}N_8)$, II.

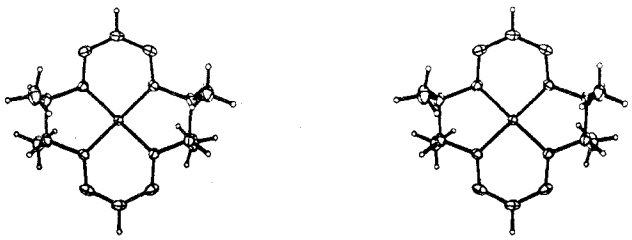

Figure 3. Stereo diagram of $Ni(C_{10}H_{18}N_8)$, viewed normal to the molecular plane, illustrating the chelate ring conformations.

Table IX. Interatomic Bond Distances (Å) and Angles (deg) for $[Ni(C_{10}H_{18}N_8)]$

		Distances	
Ni-N1	1.806 (2)	N3-N4	1.293 (3)
Ni-N4	1.809 (2)	N4-C4	1.484 (3)
N1-N2	1.293 (3)	C1-C2	1.509 (4)
N1-C2	1.477 (3)	C2-C4′ [a]	1.535 (4)
N2-C3	1.337 (4)	C4-C5	1.513 (4)
N3-C3	1.336 (4)		
		Angles	
N1-Ni-N4	93.48 (9)	N3-N4-C4	115.2 (2)
N1-Ni-N4′	86.52 (9)	N1-C2-C1	109.8 (2)
Ni-N1-N2	128.6 (2)	N1-C2-C4′	106.3 (2)
Ni-N1-C2	116.0 (2)	C1-C2-C4′	112.4 (3)
N2-N1-C2	115.1 (2)	N2-C3-N3	130.8 (2)
N1-N2-C3	119.1 (2)	N4-C4-C5	109.9 (2)
N4-N3-C3	119.0 (2)	N4-C4-C2′	106.0 (2)
Ni-N4-N3	128.6 (2)	C5-C4-C2′	113.4 (2)
Ni-N4-C4	116.0 (2)		

[a] Primed atoms are transformed by an inversion center.

perimental error, equivalent to the C–N distances in aromatic molecules such as pyridine.[37] The N2–C3–N3 angle, 130.8 (2)°, although wider than the 120° expected for regular six-membered rings, may be partially accounted for by the "bite-opening" necessary for optimal overlap of the donor nitrogen atoms with the metal ion. This open angle is only 2–3° wider than observed in first-row complexes with the 2,4-pentanedionato ligand. To our knowledge, this is the first report of a delocalized β-diazonato chelate linkage, which is expected to have structural and reactivity patterns similar to its β-dionato and β-diiminato analogues.

The ligand atoms of the six-membered chelate rings do not deviate significantly from planarity, the largest deviation being 0.01 Å or less (Table X). However, the gauche conformation of the saturated five-membered rings forces significant torsion

Table X. Distances Deviated from the Least-Squares Plane[a] of the 14-Membered Ring for $[Ni(C_{10}H_{18}N_8)]$ (Å)

Ni	0.000	C1	−1.725
N1	−0.023	C2	−0.258
N2	0.035	C3	0.091
N3	0.028	C4	−0.248
N4	−0.034	C5	−1.708

[a] The equation of the least-squares plane is $-5.044X + 7.868Y + 4.131Z = 0$.

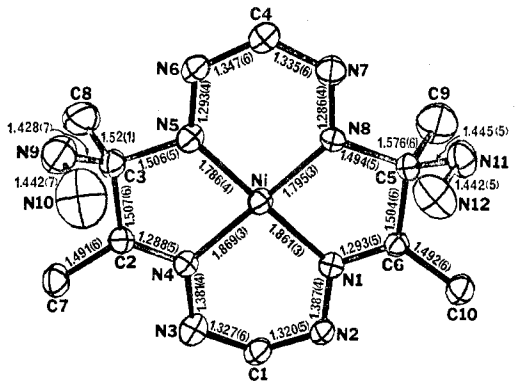

Figure 4. Molecular structure (ORTEP plot, showing 20% probability contours), labeling scheme, and interatomic distances of the macrocyclic complex $Ni(C_{10}H_{20}N_{12})$, III.

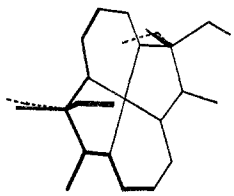

Figure 5. Diagram illustrating the nature of the disorder of the methyl and hydrazine substituents of atoms C4 and C2 in III.

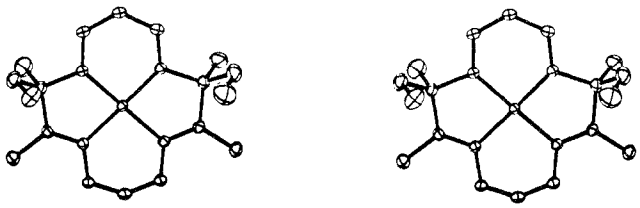

Figure 6. Stereo diagram of the $Ni(C_{10}H_{20}N_{12})$ molecule viewed normal to the molecular plane.

angles (4–8°, Table XI) in the six-membered rings. The effect of torsion angles in delocalized six-membered rings has been shown in macrocycles containing the 2,4-pentanediiminato chelate ring. For the macrocycle $Me_4Bzo_2[14]hexenatoN_4$ the Mn^{II} and Fe^{III} complexes have average imine bond torsion angles of 1.6 and 3.2°, respectively, in the β-diiminato rings. These angles do not lead to any unusual reactivity. However, in the Co^{III} complex the average angle is 12.1° and addition of oxygen, nitriles, and alkynes occurs at the apical carbon.[33,34] Thus the average N=N torsion angle of 7.0° in II may well account for the observed enhanced nucleophilicity of the apical carbon.

Structure of $[Ni(C_{10}H_{20}N_{12})]$, III. The structure consists of molecular units of an octaaza macrocyclic nickel(II) complex held together by van der Waals forces. A hydrazine substituent is attached to a carbon atom of each five-membered chelate ring. Each six-membered ring is totally unsaturated, is nominally planar, and has a negative charge dispersed over it although the delocalization pattern is markedly different in the two rings. An ORTEP plot of the molecule, with the labeling scheme and bond lengths, is presented in Figure 4. Bond

Table XI. Torsion Angles (deg) for Four-Atom Segments around the Macrocyclic Ligand

$[Ni(C_{10}H_{20}N_{12})]$		$[Ni(C_{10}H_{18}N_8)]^a$	
C6-N1-N2-C1	2.59	C4′-C2-N1-N2	21.82
N1-N2-C1-N3	2.28	C2-N1-N2-C3	7.59
N2-C1-N3-N4	1.06	N1-N2-C3-N3	3.94
C1-N3-N4-C2	1.48	N2-C3-N3-N4	3.77
N3-N4-C2-C3	0.38	C3-N3-N4-C4	6.35
N4-C2-C3-N5	1.88	N3-N4-C4-C2′	21.97
C2-C3-N5-N6	0.84	N4-C4-C2′-N1′	31.07
C3-N5-N6-C4	1.02		
N5-N6-C4-N7	0.66		
N6-C4-N7-N8	1.01		
C4-N7-N8-C5	0.20		
N7-N8-C5-C6	4.30		
N8-C5-C6-N1	6.30		
C5-C6-N1-N2	2.54		

[a] Primed atoms have been transformed by the inversion center occupied by the Ni atom.

Table XII. Bond Angles (deg) for $[Ni(C_{10}H_{20}N_{12})]$

N1-Ni-N4	95.2 (2)	C2-C3-C8	110.2 (5)
N1-Ni-N5	177.4 (2)	N5-C3-C8	110.2 (7)
N1-Ni-N8	85.6 (2)	C3-N9-N10	112.9 (5)
N4-Ni-N5	85.7 (2)	N6-N5-C3	114.1 (4)
N4-Ni-N8	178.5 (2)	N6-N5-Ni	129.0 (3)
N5-Ni-N8	93.5 (2)	C3-N5-Ni	116.8 (3)
C6-N1-N2	117.2 (4)	N5-N6-C4	119.6 (4)
C6-N1-Ni	115.9 (3)	N6-C4-N7	129.2 (4)
N2-N1-Ni	126.9 (3)	C4-N7-N8	119.6 (4)
C1-N2-N1	115.8 (4)	N7-N8-C5	113.9 (4)
N2-C1-N3	139.4 (4)	N7-N8-Ni	129.2 (3)
C1-N3-N4	116.1 (4)	C5-N8-Ni	116.8 (3)
C2-N4-N3	117.4 (4)	N11-C5-N8	113.3 (4)
C2-N4-Ni	116.1 (3)	N11-C5-C6	112.1 (4)
N3-N4-Ni	126.6 (3)	N11-C5-C9	107.7 (4)
N4-C2-C7	125.0 (4)	N8-C5-C6	104.6 (4)
N4-C2-C3	116.8 (4)	N8-C5-C9	108.5 (4)
C7-C2-C3	118.2 (4)	C6-C5-C9	110.6 (4)
N9-C3-C2	113.7 (5)	N12-N11-C5	110.4 (4)
N9-C3-N5	114.3 (4)	N1-C6-C10	123.9 (4)
N9-C3-C8	114.0 (9)	N1-C6-C5	116.8 (4)
C2-C3-N5	104.5 (4)	C10-C6-C5	119.3 (4)

Table XIII. Distances Deviated from the Least-Squares Plane[a] Defined by the 14-Membered Ring for $[Ni(C_{10}H_{20}N_{12})]$ (Å)

Ni	−0.013 (1)	N12	2.343
N1	0.017 (3)	C1	0.020 (5)
N2	0.041 (4)	C2	0.041 (4)
N3	0.017 (4)	C3	0.030 (5)
N4	0.014 (4)	C4	0.034 (5)
N5	0.035 (4)	C5	−0.003 (5)
N6	0.046 (4)	C6	0.085 (4)
N7	0.022 (4)	C7	0.072
N8	0.003 (3)	C8	−1.240
N9	1.085	C9	−1.362
N10	2.392	C10	0.263
N11	1.070		

[a] The equation of the least-squares plane is $-0.978X + 8.740Y + 9.530Z - 1.800 = 0$.

angles are listed in Table XII and deviations from the ligand plane in Table XIII. Figure 5 illustrates the nature of the disorder found in the structure. Figure 6 shows a stereoview of the molecule and Figure 7 shows the arrangement of the molecules in the unit cell.

The bond distances within the two six-membered rings are consistent with two types of delocalization. The six-membered ring Ni–N5–N6–C(4)–N(7)–N(8) is completely delocalized and has bond parameters virtually identical with those of II, the structure just previously described. This delocalized system is isolated from the seven-atom conjugated system C(6)–N1–N2–Cl–N3–N4–C2, which includes the imine functions of the five-membered chelate rings, by the tetrahedral carbon

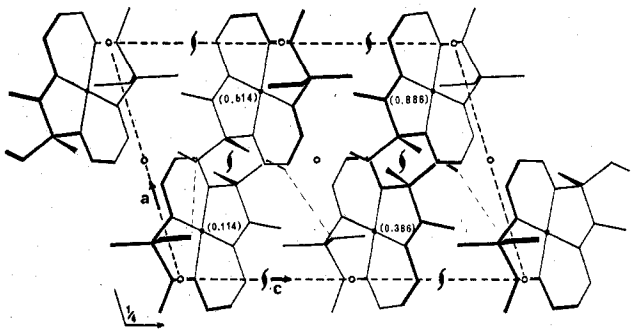

Figure 7. Projection down the *b* crystal axis illustrating the arrangement of the $Ni(C_{10}H_{20}N_{12})$ molecules in the unit cell.

Table XIV. Angles Involving Apical Carbon Atoms of Delocalized Six-Membered Chelate Rings in Some Representative Macrocyclic Complexes

complex	angle, deg	metal–nitrogen dist, Å	ref
$[Ni(C_{10}H_{20}N_{12})]$, III	129.2, 139.4[a]	1.790, 1.865	this work
$[Ni(C_{10}H_{18}N_8)]$, II	130.8	1.807	this work
$[Ni(C_{10}H_{14}N_8)]_2$, IV	135.3	1.856	41
$[Ni(C_{14}H_{18}N_4)]_2^{2+}$	128.8	1.874	40
$[Ni(C_{18}H_{14}N_4)]$	124.0	1.870	42
$[Ni(C_{10}H_{14}N_8)]$, XIII	128.50	1.784, 1.820	41
$[Co(C_{10}H_{14}N_8)(Me)(MeNHNH_2)]$, XIV	140.0	1.868	39

[a] Two different types of unsaturation are present in the six-membered rings. Average values are given when chemically equivalent chelate rings are present.

atoms C3 and C5. Although this double-bond system is conjugated, it is best described as a six-membered ring formally containing one double bond and a negative charge delocalized over a three-atom allylic-like N–C–N⁻ system and the two isolated imine functions. The hydrazine linkages, N3–N4 and N1–N2, appear to insulate the three-atom allylic-like system from the imine linkages, N4–C2 and N1–C6, of the five-membered rings. This is indicated by the average length of the latter imine bonds, 1.290 (5) Å, which do not differ significantly from isolated imine functions. Also the N–N distances, 1.384 (4) Å, in this six-membered ring are significantly longer, 0.10 Å, than in the delocalized six-membered ring opposite it.

The two different delocalization patterns yield two different types of N donor atoms as clearly reflected in the corresponding Ni–N bond distances. The completely delocalized system apparently leads to stronger Ni–N bonding and yields remarkably short Ni–N bonds, 1.790 Å compared to the chelate rings with allylic-type delocalization for which the Ni–N bond length is 1.865 (3) Å, 0.08 Å longer. The Ni–N bond lengths of a number of related highly unsaturated macrocyclic complexes are listed in Table XIV. These are all markedly shorter than observed in low-spin Ni^{II} complexes derived from saturated amines, which are typically near 2.0 Å.[38]

The different delocalization patterns of the six-membered rings have a marked effect on the bond angles of the methine atoms, C1 and C4. The fully delocalized six-membered ring has a N6–C4–N7 angle of 129.2 (4)°. For the allylic-type N3–C1–N2 assemblage, the angle widens a full 10° to 139.4 (4)°. This unusually wide angle was also observed in the related Co(III) complex XIV having the same delocalization pattern in the six-membered rings.[39] A comparison of the angles involving the apical carbon atom in a number of un-

saturated six-membered rings of macrocyclic complexes is given in Table XIV. We conclude that an angle of near 140° is intrinsic to six-membered chelate rings containing –N–C–N– linkages and is not related in any way to the "bite" of the chelate required for optimal metal–ligand interactions.

The presence of the saturated atoms, C3 and C5, in the five-membered chelate rings does not induce a significant amount of strain in the six-membered rings as revealed by the torsion angles. The torsion angles (Table XI) are all small; the largest involving atoms in the six-membered rings is 2.5°. Similarly, the presence of the extensive conjugated systems does not induce any unreasonably large angular distortions involving C3 or C5. The smallest angle is C2–C3–N5, 104.5 (4)°; the largest is N9–C3–N5, 114.3 (4)°. Such small distortions are not expected to lead to enhanced reactivity.

Conclusions

In this paper we have presented two structures containing the previously unknown delocalized β-diazonato chelate ring, which is structurally similar to the β-dionato and β-diiminato rings and which shows increased nucleophilicity at the apical carbon when strained. This resonance structure remains intact upon oxidation of the 14-membered ring to a 16π-electron system in the nickel complex provided bulky groups such as trityl prevent cofacial approach of pairs of the complex. No rearrangement to the α-diimine resonance form observed in the cobalt(III) alkyl complex occurs. Thus it is shown that different metal coordination and substituents can stabilize different resonance isomers of the dihydrooctaaza[14]annulene macrocycle.

Acknowledgment. We thank Dr. Barry Garrett for his assistance in obtaining the ESR spectra. This research was supported in part by the National Institutes of Health, Grant No. HL 14827.

Registry No. I, 60086-90-0; II, 67891-14-9; III, 67891-15-0; V, 67891-16-1; VII, 67891-17-2; VIII, 64057-23-4; IX, 67891-18-3; X, 67891-19-4; XI, 67891-20-7; XIII, 67891-21-8; Ph_3CBF_4, 341-02-6.

Supplementary Material Available: Tables listing observed and calculated structure factors for $Ni(C_{10}H_{18}N_8)$ and $Ni(C_{10}H_{20}N_{12})$ (20 pages). Ordering information is given on any current masthead page.

References and Notes

(1) To whom correspondence should be addressed at The Florida State University.
(2) T. J. Truex and R. H. Holm, *J. Am. Chem. Soc.*, **94**, 4529 (1972).
(3) N. F. Curtis, *Chem. Commun.*, 881 (1966).
(4) N. F. Curtis, *J. Chem. Soc. A*, 2835 (1971).
(5) E. K. Barefield and D. H. Busch, *Inorg. Chem.*, **10**, 108 (1971).
(6) C. J. Hipp, L. F. Lindoy, and D. H. Busch, *Inorg. Chem.*, **11**, 1988 (1972).
(7) J. C. Dabrowiak, F. V. Lovecchio, V. L. Goedken, and D. H. Busch, *J. Am. Chem. Soc.*, **94**, 5502 (1972).
(8) V. L. Goedken and D. H. Busch, *J. Am. Chem. Soc.*, **94**, 7355 (1972).
(9) S. C. Tang and R. H. Holm, *J. Am. Chem. Soc.*, **97**, 3359 (1975).
(10) B. Durham, T. J. Anderson, J. A. Switzer, J. F. Endicott, and J. F. Glick, *Inorg. Chem.*, **16**, 271 (1977).
(11) D. H. Busch, K. Farmery, V. L. Goedken, V. Katovic, A. C. Melnyk, C. R. Sperati, and N. Tokel, *Adv. Chem. Ser.*, **No. 100**, 44 (1971).
(12) L. G. Warner and D. H. Busch, *J. Am. Chem. Soc.*, **95**, 4092 (1969).
(13) L. T. Taylor, F. L. Urbach, and D. H. Busch, *J. Am. Chem. Soc.*, **91**, 1072 (1969).
(14) V. Katovič, L. T. Taylor, and D. H. Busch, *J. Am. Chem. Soc.*, **91**, 2122 (1969).
(15) D. H. Pillsbury and D. H. Busch, *J. Am. Chem. Soc.*, **98**, 7836 (1976), and references cited therein.
(16) W. R. McWhinnie, J. D. Miller, and J. B. Watts, *Chem. Commun.*, 629 (1971).
(17) S. E. Diamond, G. M. Tom, and H. Taube, *J. Am. Chem. Soc.*, **97**, 2661 (1975).
(18) G. W. Watt and P. W. Alexander, *Inorg. Chem.*, **7**, 537 (1968); G. W. Watt and D. H. Carter, *ibid.*, **7**, 2451 (1968); G. W. Watt and J. F. Knifton, *ibid.*, **7**, 1159 (1968).
(19) R. Mason, K. M. Thomas, A. R. Galbraith, and B. Shaw, *J. Chem. Soc., Chem. Commun.*, 297 (1973).
(20) C. M. Harris and E. D. McKenzie, *Nature (London)*, **196**, 670 (1962).
(21) J. P. Coleman, *Angew. Chem., Int. Ed. Engl.*, **4**, 132 (1965).
(22) J. P. Coleman, *Inorg. Chem.*, **2**, 576 (1963).
(23) V. L. Goedken and S.-M. Peng, *J. Chem. Soc., Chem. Commun.*, 62 (1973).
(24) S.-M. Peng, G. C. Gordon, and V. L. Goedken, *Inorg. Chem.*, **17**, 119 (1978).
(25) S.-M. Peng and V. L. Goedken, *J. Am. Chem. Soc.*, **98**, 8500 (1976).
(26) S.-M. Peng and V. L. Goedken, *Inorg. Chem.*, **17**, 820 (1978).
(27) "International Tables for X-ray Crystallography", Vol. I, 2nd ed., Kynoch Press, Birmingham, England, p 89.
(28) The obtainment of the refined lattice constants and the data collection were facilitated by the automatic diffractometer control program of Lenhert: P. G. Lenhert, *J. Appl. Crystallogr.*, **8**, 568 (1975).
(29) W. Busing and H. A. Levy, *J. Chem. Phys.*, **26**, 563 (1957); P. W. R. Corfield, R. Doedens, and J. A. Ibers, *Inorg. Chem.*, **6**, 197 (1967).
(30) Computations were performed on an IBM 370 computer with the aid of the following programs: Zalkin's FORDAP Fourier Program, Busing and Levy's ORFEE function and error program, and Ibers' NUCLS least-squares program. Plots of the structures were drawn with the aid of C. K. Johnson's ORTEP.
(31) Neutral atom scattering factors were taken from D. T. Cromer and J. B. Mann, *Acta Crystallogr., Sect. A*, **24**, 321 (1968). Hydrogen atom scattering factors were taken from "International Tables for X-ray Crystallography", Vol. III, Kynoch Press, Birmingham, England, 1962.
(32) R. G. Parr and B. L. Crawford, Jr., *J. Chem. Phys.*, **16**, 526 (1948); M. J. S. Dewar, *J. Am. Chem. Soc.*, **74**, 3345 (1952).
(33) M. C. Weiss and V. L. Goedken, *J. Am. Chem. Soc.*, **98**, 3389 (1976).
(34) M. C. Weiss, B. Bursten, S. Peng, and V. L. Goedken, *J. Am. Chem. Soc.*, **98**, 8021 (1976).
(35) F. V. Lovecchio, E. S. Gore, and D. H. Busch, *J. Am. Chem. Soc.*, **96**, 3109 (1974).
(36) F. A. Cotton and G. Wilkinson in "Advanced Inorganic Chemistry", Interscience, New York, N.Y., 1972, p 364; C. A. Coulson in "Valence", Oxford University Press, Amen House, London, 1963, p 188.
(37) R. C. Elder, *Inorg. Chem.*, **7**, 117, 2320 (1968).
(38) M. F. Bailey and I. E. Maxwell, *J. Chem. Soc., Dalton Trans.*, 938 (1972).
(39) V. L. Goedken and S.-M. Peng, *J. Chem. Soc., Chem. Commun.*, 258 (1975).
(40) S.-M. Peng, R. H. Holm, M. Millar, and J. A. Ibers, *J. Am Chem. Soc.*, **98**, 8037 (1976).
(41) S.-M. Peng and V. L. Goedken, *J. Am. Chem. Soc.*, **98**, 8500 (1976).
(42) M. C. Weiss, G. C. Gordon, and V. L. Goedken, *Inorg. Chem.*, **16**, 305 (1977).

Contribution from the IBM Research Laboratory, San Jose, California 95193

Mixed Sulfur–Nitrogen–Selenium Compounds

G. WOLMERSHÄUSER, C. R. BRULET, and G. B. STREET*

Received May 17, 1978

Se_4N_4 has been prepared in a new phase isostructural with S_4N_4. Its structure is reported together with the synthesis of two mixed sulfur–selenium–nitrogen compounds $(SSe_2N_2^+)_2(X^-)_2$ (X = Cl, Br). The proposed structure of the latter compounds is based on mass spectroscopic, IR, and ESR data. The existence of these mixed sulfur–nitrogen–selenium compounds is of particular significance in view of the attempts to prepare $(SeN)_x$, the analogue of superconducting $(SN)_x$.

Introduction

There have been many attempts to synthesize analogues of the superconducting polymer $(SN)_x$.[1] We have previously described short-chain oligomers involving polythiazyl chains as high as S_5N_4.[2] In contrast to $(SN)_x$ and its halogen modifications[3] these oligomers were not conducting. Extensive

0020-1669/78/1317-3586$01.00/0